Biomedical Microdevices (2020) 22: 48
https://doi.org/10.1007/s10544-020-00503-6

Microfluidic Chip based direct triple antibody immunoassay for monitoring patient comparative response to leukemia treatment

Kutay İçöz[1,2] · Ünal Akar[2] · Ekrem Ünal[3]

Published online: 13 July 2020

Abstract
We report a time and cost-efficient microfluidic chip for screening the leukemia cells having three specific antigens. In this method, the target blast cells are double sorted with immunomagnetic beads and captured by the 3rd antibody immobilized on the gold surface in a microfluidic chip. The captured blast cells in the chip were imaged using a bright-field optical microscope and images were analyzed to quantify the cells. First sorting was performed with nano size immunomagnetic beads and followed by 2nd sorting where micron size immunomagnetic beads were used. The low-cost microfluidic platform is made of PMMA and glass including micro size gold pads. The developed microfluidic platform was optimized with cultured B type lymphoblast cells and tested with the samples of leukemia patients. The 8 bone marrow samples of 4 leukemia patients on the initial diagnosis and on the 15th day after the start of the chemotherapy treatment were tested both with the developed microfluidic platform and the flow cytometry. A 99% statistical agreement between the two methods shows that the microfluidic chip is able to monitor the decrease in the number of blast cells due to the chemotherapy. The experiments with the patient samples demonstrate that the developed system can perform relative measurements and have a potential to monitor the patient response to the applied therapy and to enable personalized dose adjustment.

Keywords Magnetic micro/nano particles · Immunoassay · Biochip · Leukemia · Direct triple antibody · Microfluidic -based monitoring; comparative response

1 Introduction

Acute lymphoblastic leukemia (ALL) is the most common type of cancer among children in the United States (Siegel et al., 2017). ALL is divided into two subtypes; B precursor (B-ALL), and T precursor (T-ALL) according to the origination. 85% of the children with ALL arise from B cells, whereas %15 of them originates from T cells (Chiaretti et al., 2014).

B-ALL has four main stages based on the maturation of cells; pro-B, common B, pre-B and immature B. The gene expression and cell surface markers at stages display significant heterogeneity. For example, CD19 is a membrane antigen and highly expressed in all stages of ALL, whereas the presence of CD10 antigen defines common ALL (Chiaretti et al., 2014). The expression of cell surface markers show variations at each stage and also changes in cell surface markers as an impact of therapy were reported (Wood, 2015).

Chemotherapy, bone marrow transplantation, radiation treatment and immunotherapy are the different treatments for leukemia. Among these methods, chemotherapy is the major treatment method, but responses may differ from patient to patient (Terwilliger & Abdul-Hay, 2017). For instance, if the chemotherapy is successful, patients achieve remission. On the other hand, if the cancer cells are resistant to treatment, these cells can cause relapses and repeat the cancer. This condition is called Minimal Residual Disease (MRD) (Hauwel & Matthes, 2014) and current international treatment protocols require monitoring the minimal residual disease (MRD) for the ALL patients. The 15th day of the chemotherapy treatment is a check point for the assessment and in the case of positive MRD detection, intensive chemotherapy is used (Campana, 2009).

Electronic supplementary material The online version of this article (https://doi.org/10.1007/s10544-020-00503-6) contains supplementary material, which is available to authorized users.

✉ Kutay İçöz
kutay.icoz@agu.edu.tr

[1] BioMINDS (Bio Micro/Nano Devices and Sensors) Lab, Department of Electrical and Electronics Engineering, Abdullah Gül University, 38080 Kayseri, Turkey

[2] Bioengineering Department, Abdullah Gül University, 38080 Kayseri, Turkey

[3] Pediatric Hematology Department, Erciyes University, 38030 Kayseri, Turkey

Nowadays, Flow Cytometry (FC), Polymerase Chain Reaction (PCR), fluorescence in situ hybridization (FISH) are the laboratory techniques used for MRD detection (Hauwel & Matthes, 2014; Øbro et al., 2012). These methods are time and cost inefficient and require trained personnel to operate in a certified laboratory. In western countries, monitoring patients for possible relapses is becoming a routine (Hauwel & Matthes, 2014). However, in many countries, patients do not have access to such facilities. Using only one type of cell-surface marker to detect the blast cells that are resistive to chemotherapy is not sufficient thus FC techniques for MRD monitoring is based on detecting multiple cell-surface markers (Lucio et al., 2001)–(Gaipa et al., 2013). CD19, CD34 and CD10 can be used to detect immature cells but additional markers such as CD45, CD38, CD15, CD33, CD58 are needed to identify leukemia (Gaipa et al., 2013).

Microfluidic systems have great advantages such as being low-cost, requiring less samples and low energy (Alapan et al., 2015). Numerous microfluidic platforms have been developed to solve various cancer related problems such as detection of circulating tumor cells for early diagnosis of cancer (Huang et al., 2015), in vitro modelling of cancer cells to investigate the behavior (Ozcelikkale et al., 2017), adoptive cell therapies to destroy cancer cells (Adriani et al., 2016), examination of chemotherapy resistance (Islam et al., 2018). A microfluidic system for detecting MRD in patients with acute myeloid leukemia (AML) was described recently in 2016 (Jackson et al., 2016). This microfluidic system is composed of sinusoidal flow channels and detection method incorporates fluorescent and nuclear staining which requires fluorescence microscopy for imaging.

Immunomagnetic particles have been used for capturing and separating target molecules to transport them into reduced volume of buffer solutions. Thus, interfering other molecules are eliminated and target molecules are concentrated into desired microsystems and usually sandwich assays are generated (Icoz & Savran, 2010). Screening cells for two surface markers was demonstrated in (Sun et al., 2017) where both 4.5 μm size immunomagnetic particles and 4.95 μm size non-magnetic beads were sequentially applied to cells and cells that are CD44+/CD24- were separated from the mixture of cells that are CD44+/CD24+, CD44-/CD24+, CD44-/CD24-, CD44+/CD24-. A permanent magnet and a microfluidic chip were used to apply an external magnetic field for immunomagnetic separation and immobilizing cells for imaging (Sun et al., 2017).

In our previous work (İçöz et al., n.d.), we investigated the capture efficiency of immuno-magnetic particles of micrometer size and nanometer size for the cultured cells without a third capture in a microfluidic platform. We found that double sorting has a capture yield of 95–98% which is the recovery rate of target cells from the pure cell population (B-ALL cell culture). In this study, the main idea is to capture and separate B-ALL cells of patients by using multiple biomarkers. For that purpose, CD10, CD19, and CD45 antibodies were chosen to directly capture and detect the target cells. Our design consists of using both micro and nano size immunomagnetic beads. The micro size immunomagnetic beads are visible under the bright-field optical microscope and thus, simultaneously serve following two purposes: 1) as immunomagnetic separation agents and 2) as visual labels for target cell identification from the acquired images. Even though the nano size immunomagnetic beads are not visible under the bright-field optical microscope, they serve two purposes: 1) as immunomagnetic separation agents and 2) magnetic separator system used for nano size beads provides magnetic selectivity.

The magnetic rack used to separate micron size beads did not generate enough magnetic force to pull nano size beads, we used this feature for selectivity between the magnetic beads. We first performed separation with nano size immunomagnetic beads and then performed separation with micro size immunomagnetic beads (Fig. 1). This magnetic selectivity and double sorting provided separation of cells that are CD10+/CD19+ but not CD10+/CD19- or CD10-/CD19+. Previously, we compared the efficiencies of the surface modification methods to capture B-ALL cells on gold surfaces (Icoz et al., 2018).

In this work we combine the results of the previous studies to screen B-ALL cells having three surface markers simultaneously. We present a microfluidic system housing micron size gold pads for capturing cells that are previously double sorted by immunomagnetic particles. In the next sections we detailed the experimental procedure and described the low-cost microfluidic platform. Both cultured cells and cells from 8 samples of 4 patients were examined using the developed system. We compared the performance of the system with flow cytometry as gold standard.

2 Materials and methods

2.1 Detection strategy

The detection strategy is illustrated in Fig. 1, first double immunomagnetic sorting is implemented for the screening of two surface markers on the cell membrane. The mixture of captured cells and beads is flowed through the microfluidic system. The microfluidic system consists of four different layers: a glass layer for bottom fluid cover, a glass slide having an array of gold pads, polymethylmethacrylate (PMMA) channel, and a PMMA top fluid cover. The gold pads were functionalized with antibodies to capture target cells. A bright-field optical microscope (Nikon) equipped with a charge-coupled (CCD) camera was used to record the images.

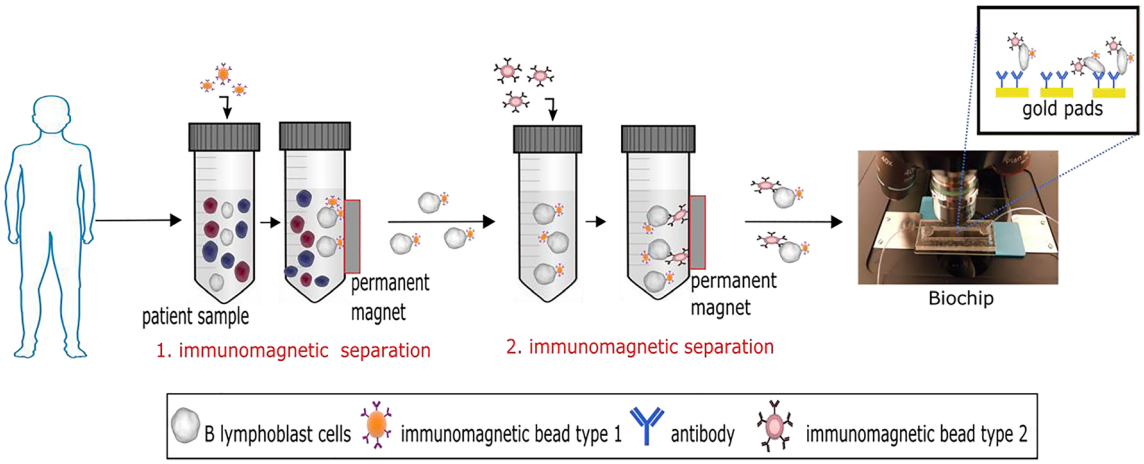

Fig. 1 Schematic illustration of the detection strategy. The target cells are first captured and separated by nano size magnetic beads conjugated with CD10 antibody. The second sorting is performed with micron size magnetic beads conjugated with CD19 antibody. The double sorted cells are introduced to the microfluidic system where gold pads are functionalized with CD45 antibody

2.2 Preparation of the microfluidic Chip

The microfluidic device consists of four components. The bottom glass cover is a standard microscope slide. The middle channel layer and top cover is Polymethyl methacrylate (PMMA) which was purchased from Mc Master Carr (Elmhurst, IL). The design of the microfluidic system was sketched using CorelDRAW (X7) and then a laser cutter (Epilog Zing Laser Series) was used to define the PMMA channel and the inlet, outlet ports on the top cover. The gold pads were fabricated on a 6-in. glass wafer using standard lithography, deposition and lift-off process. In our previous study using the cell culture (Uslu et al., 2019), we observed that the average size of a cell is around 20–25 μm. To capture one or two cells on a single micropad, initially 25 μm × 25 μm size was considered. Also, smaller and larger micropads were placed on the photolithography mask to experimentally test the capture efficiency. The micropads were deposited on glass wafer by sputtering a 25 nm titanium adhesion layer and 100 nm gold layer. A very similar microfabrication process was detailed in (Shukla et al., 2019). Arrays of different size gold pads ranging from 15 μm × 15 μm to 35 μm × 35 μm were fabricated. The glass wafer was cut into pieces of 7 mm × 10 mm and placed inside the chamber of 8 mm × 40 mm (Fig. 2). A double-sided tape (Ve-ge tapes, Turkey) used for sealing whole system and inlet-outlet tubing was sealed with epoxy. The height of the channel is 1 mm due to the thickness of the middle PMMA layer. One peristaltic pump at the inlet injects fluid and a syringe pump at the outlet pulls the fluid at a rate of 10 μL/min.

2.3 Chip surface functionalization

The details of the surface functionalization procedure was reported in a previous publication (Icoz et al., 2018). The protein G was purchased from Thermo-Fisher (Waltham, MA). The CD45 antibody was purchased from BioLegend (SanDiego, CA) and all other chemicals were purchased from Sigma-Aldrich (St.Louis, MO).

Briefly the glass slide with the gold pads were rinsed with deionized water and absolute ethanol and then dried under a nitrogen stream. Then the chip surface was modified with 1 mM 11-Mercaptoundecanoic acid (MUA) in ethanol for 24 h and rinsed with absolute ethanol for 2 min. EDC/NHS was used as a cross-linker in the experiments. For the N-Ethyl-N′-(3-dimethylaminopropyl) carbodiimide hydrochloride (EDC)/ N-hydroxysulfosuccinimide (NHS) crosslinking, the surface was treated with the solution of 5 mg EDC, 5 mg NHS in 1 mL deionized water for 25 min, and the surface was rinsed with deionized water for 2 min. Subsequently, the protein G solution, 800 μL protein G (5% protein G solution in deionized water) in 5.4 mL Phosphate Buffered Saline (PBS) was added on the chip surface for 25 min, and then surface rinsed with PBS for 2 min. The 510 μL of stock solution of CD45 (20 μL CD45 antibody in 1 mL PBS) was diluted in 5.4 mL PBS and then the solution of CD45 was put on the surface for 25 min, followed by PBS. The last step before adding cells was Bovine Serum Albumin (BSA) blocking where 5% BSA solution was added on the surface for 120 min to prevent non-specific bindings of cells.

2.4 Preparation of Immunomagnetic beads

We followed the same experimental procedure of double sorting reported in (İçöz et al., n.d.). Superparamagnetic beads of 120 nm in diameter coupled with monoclonal anti-human antibody were purchased from Miltenyi Biotec (Auburn, CA) and beads of 4.5 μm in diameter coupled with monoclonal anti-human antibody were purchased from Dynabeads, Thermo-Fisher (Waltham, MA). Briefly, a washing buffer

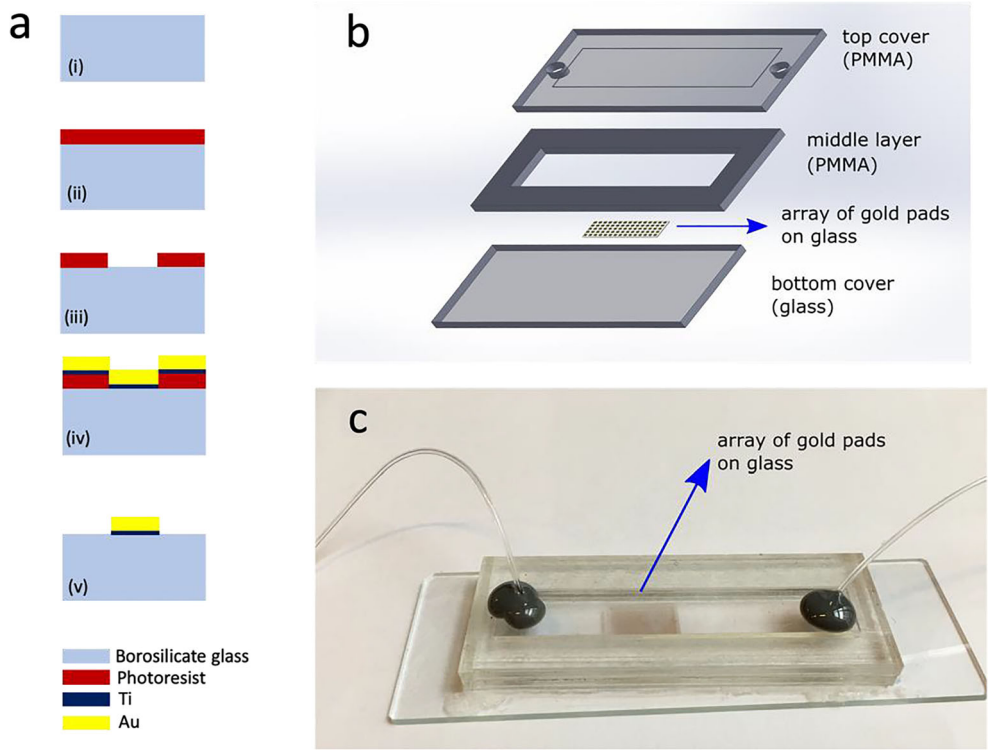

Fig. 2 (a) Microfabrication process flow for the array of gold pads: i) borosilicate glass wafer cleaning, (ii) spin coating of photoresist, (iii) patterning photoresist, (iv) titanium and gold deposition (v) lift off process (b) Exploded illustration of the of the microfluidic chip (c) The assembled device. Blue arrows indicate the array of gold pads on glass

was prepared, 25 μL of micro size immunomagnetic beads and 20 μL of nano size immunomagnetic beads were incubated with the cells and specific magnetic separation systems were used for applying the external magnetic field. According to the manufacturer, the magnetic column separator induces a high-gradient magnetic field (10,000 fold amplification) to separate the nano size immunomagnetic beads (Miltenyi Biotec, n.d.). On the other hand, the magnetic separation rack (New England Biolabs part # S1506) used for micro size immunomagnetic beads does not produce enough magnetic field to attract nano size immunomagnetic beads (we also experimentally observed this fact). We measured a magnetic field of 100–300 mT for the magnetic separation rack of micro size beads and 500 mT for the magnet (Miltenyi Biotec part #130–042-102) of the nano size bead separator without the column. According to manufacturer (Miltenyi Biotec) this magnetic field is amplified (10,000-fold amplification) when the column (part # 130–042-201) is inserted in the separator. In other words, the permanent magnets used for separation of micro size particles do not interfere with the nano size particles.

2.5 Automated counting

In our previous study (Uslu et al., 2019), we demonstrated machine learning based image analysis methods to quantify cells, immunomagnetic beads and clusters with a precision of 91% with 40X objective and 80% with 20X objective. In a new study (Uslu et al., 2020), we improved our image analysis algorithms and included detection of micropads. The new method was able to reach an average precision of 95% for patient cells using 20X objective. The detection of immunomagnetic beads and micropads has a precision of 99%. Briefly the size, color and shape features were used to distinguish between cells, immunomagnetic beads and micropads. The average detection error for the cells attached to the micropads is 0.17. The algorithm is able identify the cells captured on the micropads. When a cell is captured on the micropad it means that it is a CD19+/CD10+/CD45+ cell, otherwise it is a CD19+/CD10+/CD45- cell. The algorithms were developed on Matlab (R2018b, The MathWorks Inc., Natick, MA), running on a work station with 2.90 GHz CPU and 8 GB RAM.

2.6 Cell culture experiments

In order to test the performance of the microfluidic platform, the first measurements were performed using the cell line (B lymphoblast cells CCRF-SB) which was purchased from ATCC (Rockville, MD). The surface markers of the cells were measured using flow cytometry FACSAriaIII, BD Biosciences, (Franklin Lakes, New Jersey) and it was found that less than 10% of the ATCC cells have CD10 antigen on the cell surface. Flow cytometry measurements also revealed that 99% of the ATCC cells have CD19 and CD45 antigens on the cell surface. For that reason, we did not perform triple antibody screening for the cell culture experiments and used

only two types of antibodies (CD19 and CD45) to capture the target cells.

To test the capture efficiency and non-specific binding we performed control experiments. Surface modification procedure consisting of MUA➔EDC/NHS➔Protein G➔Antibody➔BSA➔target cells were performed and at the antibody step either no-antibody or CD45 antibody were added and the number of cells on the surface were compared.

We also performed tests to investigate the cell capture ratio of the microfluidic platform, thus we introduced different number of cells to the platform which was modified by the above-mentioned same procedure and the captured cells on the gold pads were counted. Experiments were repeated at least 3 times and the mean values and standard deviations were calculated.

2.7 Patient samples

All bone marrow samples used in the present study were obtained under the approval of the Clinical Research Ethics Committee of the Erciyes University Faculty of Medicine (Approval date: 09/01/2015, Decision no:2015/21, Kayseri, Turkey). Written informed consent was obtained from all parents/legally authorized representatives of patients. The Declaration of Helsinki was followed throughout the study.

Pediatric patients with acute lymphoblastic leukemia were treated according to the international Berlin-Frankfurt-Münster 2009 (BFM 2009) protocol (Campbell et al., 2009) in Erciyes University Pediatric Hematology Department. Bone marrow samples of patients were collected on diagnosis and on 15th day of the chemotherapy treatment. Unlike cell culture experiments, the number of cells in the samples varied from patient to patient. The average volume of the collected bone marrow samples is 3.2 mL. The collected patient samples divided into vials of 1.5 mL for further analysis (Lowest 1.7×10^6 cells per vial to highest 7×10^6 cells per vial). As an example, from one patient 0.5 mL bone marrow collected which included 12×10^6 nucleated cells and then samples were divided into 6 vials each vial had 2×10^6 cells. The collected samples were diluted with Dulbecco's Phosphate-Buffered Saline (DPBS) at a ratio of 1–1. Then diluted sample was added to a Sepmate tube (Stemcell Technologies, Vancouver, BC) including 20 mL of Lymphocyte Separation Medium (LSM, PAA Laboratories, Austria). The mixture was centrifuged and separated cells were transferred to a sterile tube. DPBS was added to sterile tubes to obtain a volume of 50 mL. Then centrifuged again to remove supernatant and the cells were resuspended in 5 mL of DPBS. Later immunomagnetic separation protocol was applied to the cells. The double pumps as mentioned above were used to introduce the captured cells (3 mL–5 mL) to the functionalized chip surface. The captured cells were counted from the recorded bright-field microscope images.

The change of the number of blast cells from the diagnosis to 15th day is investigated by the flow cytometry and microfluidic chip. The flow cytometry counted 10,000 events for each measurements and percentages of cell populations were obtained.

All experiments were performed in room temperature, only cell cultures were stored in an incubator of 37 degree of Celsius and 5% Carbon-Dioxide.

2.8 Statistical analysis

8 samples from 4 patients were analyzed both with the developed microfluidic system and flow cytometry. The outputs of these two methods were compared using non-parametric Mann-Whitney test.

3 Results

In a previous study we optimized the immunomagnetic double sorting (İçöz et al., n.d.) and used those results in this study. Figure 3 shows the images of the gold pads and the captured cell-immunomagnetic particle complex. The images were acquired by the optical bright field microscopy and scanning electron microscopy (SEM). SEM was not performed for all samples but on some dried samples for visualization of the cells, beads and micropads. As seen in Fig. 3, there are unbound beads and cells captured with immunomagnetic beads in the microfluidics. An automated cell counting software developed in house were used for quantification (Uslu et al., 2020).

To test the performance of the low-cost microfluidic platform, we tested the whole system with the cultured cells. The results of the cell culture experiments are shown in Fig. 4. The cultured cells were first counted and then introduced to the microfluidic platform. The captured cells on the gold micropads inside the microfluidics were counted. The number of input cells were approximately 30,000, 100,000, 250,000 and 500,000 (all input cells were injected in a volume of 5 mL) which correspond to average captured cells in the microfluidics 250, 5500, 11,470 and 18,500 respectively. For the control experiment we did not add CD45 antibody but BSA and introduced approximately 500,000 cells in 5 mL to the microfluidics. These results reveal that microfluidic platform has a positive correlation response to the number of introduced cells, however, many of the introduced cells were not captured on the gold pads in the microfluidic platform. This is because the gold pads only cover an area of the 20% of the total fluidic chamber thus there is only a limited functionalized gold area that cells can specifically bind.

To increase the yield of capturing cells, the design can be modified in 2 dimensions by increasing the lay out area of the

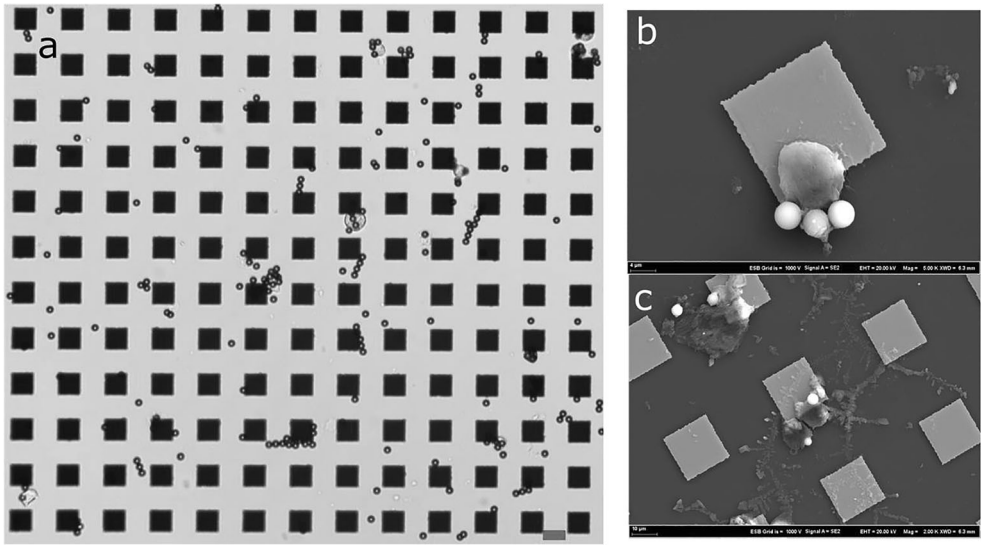

Fig. 3 (a) Bright-field optical micrograph of the array of gold pads, captured cells and immunomagnetic beads. Scale bar = 20 μm. (b), (c) Scanning electron microscopy images of the gold pads, captured leukemia cells and the immunomagnetic beads

gold pads in the microfluidic channel. Another approach to increase the yield is to fabricate 3 dimensional structures such as fabricating gold micro posts instead of pads. For the experiments in Fig. 4A, we used arrays of 26,000 gold pads for each measurement, whereas for the experiments in Fig. 4B, we used arrays of 33,000 gold pads for each measurement. The performed control experiments show the selectivity of the modified gold pads. In the case of no antibody, significant number of cells did not bind to the gold pads as expected. These results show that the functionalized gold pads serve the purpose of capturing target cells. For the sake of proof-of-principle and being low cost, we accepted the limitations of the existing microfluidics and performed the experiments without any major changes in the design.

To demonstrate the potential of the system, a total of 8 bone marrow samples (4 samples at diagnosis and 4 samples on the 15th day of the chemotherapy) from 4 leukemia patients were analyzed for three surface markers both with the developed system and the flow cytometry as the gold standard. The collected samples were divided into two vials. For the first vial, cells were immunomagnetically separated and introduced to the microfluidic platform. In the microfluidic platform the cells which were already loaded with beads, were captured on the functionalized gold pads and then cells were quantified. To find the ratio of captured cells in the chip, the number of captured cells on the pads and the total number of gold pads are used. In parallel, the second vial of the sample was analyzed with flow cytometry and the percentage of cells having three markers were identified, the FC measured 10,000 events for each measurements and percentages of cell populations were obtained (Fig. 5). In the literature when the flow cytometry measurements are performed for MRD, multiple markers such as CD38, CD20, CD10, CD19, CD34, CD58, CD45 and CD11 antigens were analyzed (Dworzak et al., 2008).

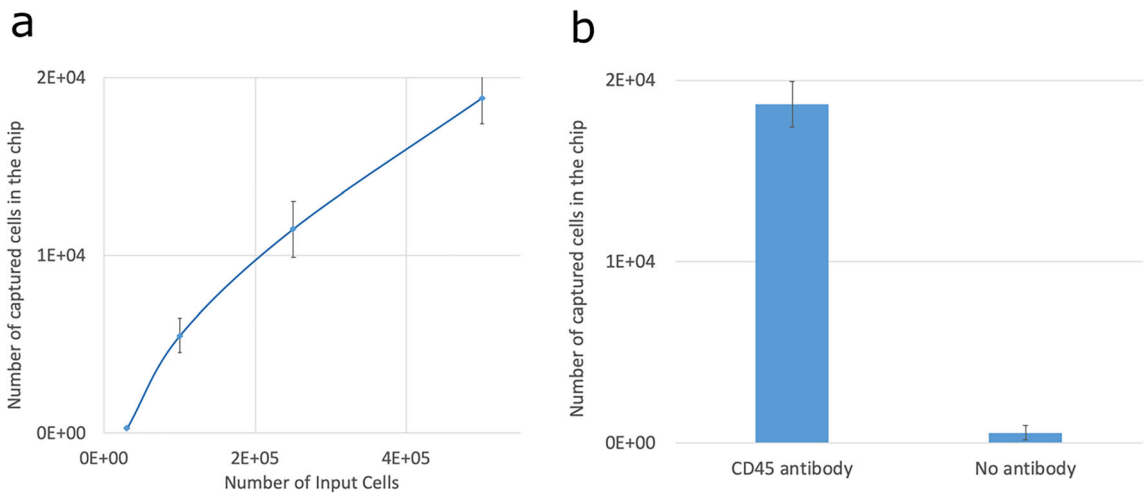

Fig. 4 Results of the cell culture experiments, (a) The number of captured cells in the microfluidic chip with respect to number of input cells (b) The control experiments with and without CD45 antibody. Error bars indicate the standard deviation from three experiments

All 4 patients show positive signs for remission and it was decided that not intensive dosage but regular dosage of chemotherapy was needed after the 15th day. To compare the results of both methods for 8 samples from 4 patients, 0.01 was considered as the statistical significance level. Mann-Whitney Test Statistics Asymp. Sig. (2 -tailed) $P = 0.564 > 0.01$ showed that both methods were 99% agreement in detecting the decrease of cells between the initial diagnosis time and the 15th day of chemotherapy. These results show the potential of the platform and it can be used to detect the patient's YES(+)/NO(−) response to the applied therapy. For the patient samples after the magnetic separation, the minimum number of cells captured in the microfluidic platform was 3153 blast cells when 20,000 target cells were introduced and the corresponding capture yield of the microfluidics was calculated as 15.7%.

4 Discussion

As seen from the Fig. 5, there are some variations between the flow cytometry and microfluidic chip readings among the patients. For example, for the measurements of the patient 2, the gold pads were in the size of 35 μm × 35 μm where some cells were on top the gold pads and difficult to count. For the patient 3, gold pads of 15 μm × 15 μm, for the patients #1 and #4, gold pads of 25 μm × 25 μm were used. The average size of the cells from the culture (20–25 μm) are bigger than the average size of the cells from the patients (10 μm), and also, we observed there were many cells in 5–8 μm size in the patient samples, as a consequence, larger gold pads are not suitable for accurate measurements. Larger micropads contain higher number of antibodies and thus can bind to cells with a higher rate. However, the larger micropads blocks the microscope light for the cells fully located in the micropad area, and as a consequence the cells is not visible and detectable by the automated counting algorithm.

We also observed that if the immunomagnetic capture and separation process has a high capture yield, compared to the capture yield in the microfluidic platform. However, for some patient samples that we did not include in this manuscript, immunomagnetic capture yield was low. This could be due to lack of the expected surface markers on the cell membrane. We assumed that all target cells have CD19, CD10 and CD45 antigens on the surface and our FC measurements only analyzed the samples for these three antigens, however, there are studies in the literature that there are exceptions (Moon et al., 2007)–(Rosenthal et al., 2017)–(Keeney et al., 2017). The immunophenotypic modulation of blast cells in ALL was previously investigated using a 8-color FC (Burnusuzov et al., 2016). The FC measurements revealed that the expression of CD10, CD19 and CD34 were downmodulated, the expression of CD20 was upmodulated and no changes were noticed for the expression of CD38, CD58 and CD45 on 15th day. These results agree with our measurements showing the decrease in the number of blast cells.

In the literature there are microfluidic platforms to detect circulating tumor cells (Nagrath et al., 2007; Zheng et al., 2011) where complex micro structures such as posts or apertures were fabricated. Our system at the current state is not capable of detecting few cells but it is a platform to monitor the differential change in number of cells by time. Unlike the microfluidic platforms that can detect few cells, the main goal of our system is to perform comparative measurements between the initial diagnosis and on the 15th day of the chemotherapy. To show the potential of the system, samples from 4 leukemia patients were analyzed. The 4 samples taken on the initial diagnosis and 4 samples on the 15th day of the chemotherapy were analyzed both with the flow cytometry and the microfluidic platform. The statistical comparison between two methods revealed that two systems produced statistically equal results in detecting the decrease of the blast cells from initial diagnosis to 15th day of chemotherapy for 4 patients. According to BFM 2009 treatment protocol, 15th day FC MRD measurements are used to classify the risk groups. Standard risk (SR) group is FC blast cell ratio < 0.1%, and high-risk (HR) group is FC blast cell ratio > 10%. We were not able to analyze samples from relapsed patients with the microfluidic platform, however we checked the medical records of previous patients at Erciyes University and found that blast cell amount on the 15th day between standard-risk and high-risk patients differ 10-fold to 10,000-fold. For a relapsed patient there were approximately 39,000 for another relapsed patient there were 18,700 blast cells in 1 mL of blood on the 15th day. On the other hand, two patients who did not relapse had 2 and 200 blast cells, respectively on the 15th day. Our measurements on patient samples revealed that the developed system was able to detect approximately 3000 blast cells and the capture yield of the microfluidics is 15.7%. If the relapsed patient samples were measured with the microfluidic platform which corresponds to 6123 and 2936 captured blast cells in the microfluidic platform, the system would be able to identify the comparative difference. However, the sensitivity has to be improved significantly so that all the risk groups including standard-risk patients can be identified and microfluidic platform can be used for clinical applications. For an early relapse patient the relative frequency of leukemic cells is more than 10^-3 (van Dongen et al., 2015).

When compared with the microfluidic system developed for monitoring MRD in AML (Jackson et al., 2016), our system does not require high-cost fluorescent microscopy for imaging and the fabrication of our microfluidic system is much simpler. A bright-field optical microscope which is easily accessible in many clinics is needed to acquire images and the developed automated image analysis method (Uslu et al., 2020) can segment the cells, immunomagnetic beads and

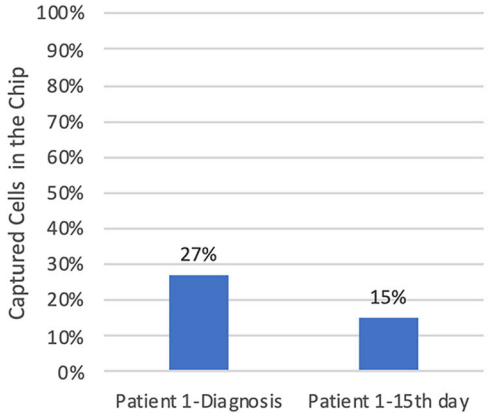
Captured Cells in the Chip
100%
90%
80%
70%
60%
50%
40%
30%
20%
10%
0%
27%
15%
Patient 1-Diagnosis
Patient 1-15th day

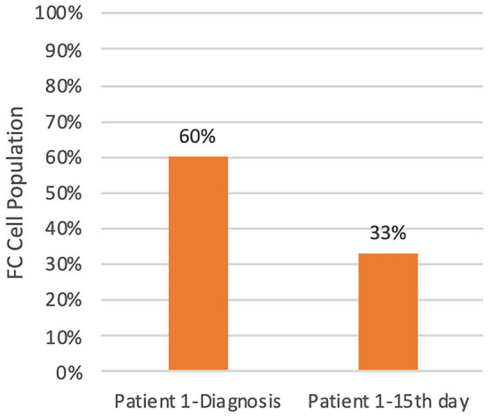
FC Cell Population
100%
90%
80%
70%
60%
50%
40%
30%
20%
10%
0%
60%
33%
Patient 1-Diagnosis
Patient 1-15th day

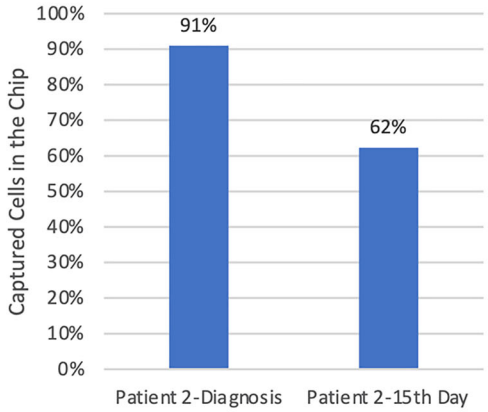
Captured Cells in the Chip
100%
90%
80%
70%
60%
50%
40%
30%
20%
10%
0%
91%
62%
Patient 2-Diagnosis
Patient 2-15th Day

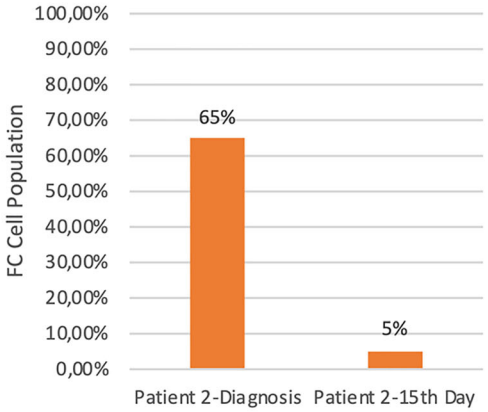
FC Cell Population
100,00%
90,00%
80,00%
70,00%
60,00%
50,00%
40,00%
30,00%
20,00%
10,00%
0,00%
65%
5%
Patient 2-Diagnosis
Patient 2-15th Day

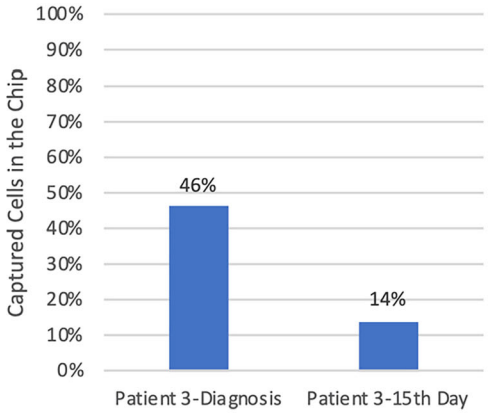
Captured Cells in the Chip
100%
90%
80%
70%
60%
50%
40%
30%
20%
10%
0%
46%
14%
Patient 3-Diagnosis
Patient 3-15th Day

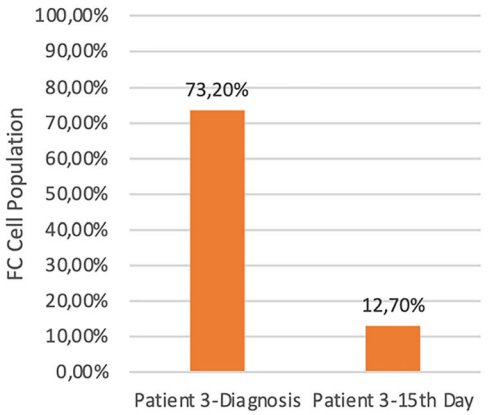
FC Cell Population
100,00%
90,00%
80,00%
70,00%
60,00%
50,00%
40,00%
30,00%
20,00%
10,00%
0,00%
73,20%
12,70%
Patient 3-Diagnosis
Patient 3-15th Day

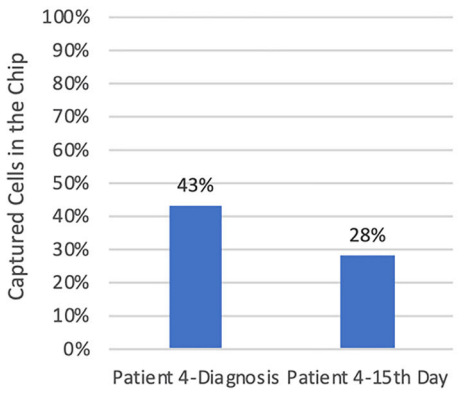
Captured Cells in the Chip
100%
90%
80%
70%
60%
50%
40%
30%
20%
10%
0%
43%
28%
Patient 4-Diagnosis
Patient 4-15th Day

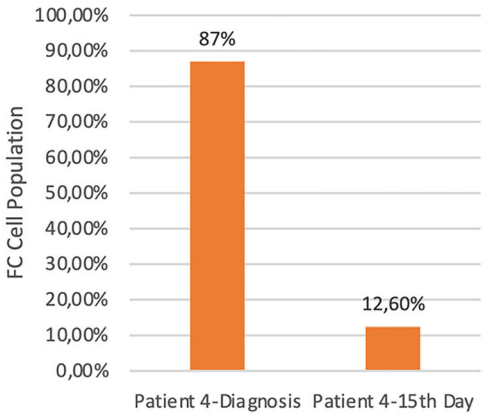
FC Cell Population
100,00%
90,00%
80,00%
70,00%
60,00%
50,00%
40,00%
30,00%
20,00%
10,00%
0,00%
87%
12,60%
Patient 4-Diagnosis
Patient 4-15th Day

◀ **Fig. 5** The analysis of 8 samples from 4 patients with the developed microfluidic chip and flow cytometry. Statistical significance was considered at $P < 0.01$ (Mann-Whitney Test Statistics Asymp. Sig. (2 - tailed) $P = 0.564 > 0.01$, there is no significant statistical difference in detecting the decrease in cell numbers)

micropads with high precision. Previously, many cell-phone microscope systems democratizing the laboratory tests have been introduced in the literature (Hernández-Neuta et al., 2019). In our previous study we demonstrated an application of cell phone microscopy to analyze immunomagnetic beads (Içöz, 2016). We believe our microfluidic system can be combined with a cell phone microscope and even the need of a standard microscope would be eliminated. Another advantage of the low-cost microfluidic platform is that it can be considered as a method to adjust the treatment dosage enabling personalized medication for low-income countries.

It was observed that capturing the target cells loaded with immunomagnetic beads has 15.7% yield whereas capturing unloaded cells has 5% yield (Fig. 4a). The loaded cells experience a higher gravitation force and move toward the floor of the microfluidics increase the interaction with the functionalized pads. Our future efforts will be on improving the sensitivity of the system, the ultimate goal of MRD monitoring is detecting 1 target cell in 10^6 cells (Hauwel & Matthes, 2014). Even though, the current system has high correlation with FC to detect the decrease in the number of cells for the samples of 4 patients, further developments are necessary to improve the performance of the system for clinical applications. The fabrication of gold pads is low-cost compared to the fabrication of 3D structures. To increase sensitivity, instead of the gold pads gold posts can be fabricated thus volume sample interaction and capture rates can be increased. Another improvement to increase cell capture performance would be to decrease the channel height and length and use durable sticking materials, thus these improvements would also allow optimizing the flow rates and decrease the non-specific binding to the glass surface. In our current design, the gold pads are the defined areas where specific binding is expected to happen. The structure of the microfluidic system can be changed to alternative designs such as using a functionalized glass surface for capturing the target cells however, this design requires counting the unbound cells at the output of the microfluidics.

5 Conclusion

We have presented a cost and time efficient microfluidic chip that demonstrates a potential to monitor the efficiency of applied therapy. The technique is based on screening target blast cells for three different surface markers. Two markers on the cells are screened with immunomagnetic beads of micron and nano size. The third type of the antibody is immobilized on the gold pads in the microfluidic platform. The immunomagnetic incubation and separation of target cells were completed in 1 h, the fluid flow in microfluidics and imaging were performed in 45 min. PMMA and glass were used to form the microfluidic platform since they are low-cost and PMMA has some production advantages compared to PDMS. The PMMA channel was formed just in seconds using a laser cutter and layers combined using a double-sided tape. The performance of the system was tested by analyzing 8 samples from 4 patients. By investigating the typical blast cells numbers, we found that the developed method is able to monitor the patient response to applied therapy for high risk group patients. We can conclude that the developed method is versatile; by changing the antibodies conjugated to immunomagnetic beads and the antibody immobilized on the gold surface, the system can be adopted to detect various cells by screening the presence of double or triple cell surface antigens. Our future efforts will be improving the sensitivity of system and testing more patient samples.

Acknowledgements Authors acknowledge TÜBİTAK (Project No: 115E020) for financial support. Authors also give thanks to Nazendenur Akşit and Ahsen Aydın for helping on taking the SEM images, Dr. Cengiz Gazeloğlu from Isparta Süleyman Demirel University for valuable discussions on statistical analysis.

Author contributions K.I designed the experiments, U. A, K. I and E. U conducted the experiments, interpreted the data and wrote the manuscript.

References

G. Adriani, A. Pavesi, A. T. Tan, A. Bertoletti, J. P. Thiery, and R. D. Kamm, "Microfluidic models for adoptive cell-mediated cancer immunotherapies," *Drug Discovery Today*. 2016

Y. Alapan, K. Icoz, U.A. Gurkan, Micro- and nanodevices integrated with biomolecular probes. Biotechnol. Adv. **33**(8), 1727–1743 (2015)

H. A. Burnusuzov *et al.*, "Immunophenotypic Modulation of the Blast Cells in Childhood Acute Lymphoblastic Leukemia Minimal Residual Disease Detection," *Folia Med. (Plovdiv).*, 2016

D. Campana, Minimal residual disease in acute lymphoblastic leukemia. Semin. Hematol. **46**(1), 100–106 (Jan. 2009)

M. Campbell *et al.*, "A Randomized Trial of the I-BFM-SG for the Management of Childhood Non-B Acute Lymphoblastic Leukemia STEERING COMMITTEE," 2009

S. Chiaretti, G. Zini, and R. Bassan, "Diagnosis and subclassification of acute lymphoblastic leukemia," *Mediterranean Journal of Hematology and Infectious Diseases*. 2014

J.J.M. van Dongen, V.H.J. van der Velden, M. Brüggemann, A. Orfao, Minimal residual disease diagnostics in acute lymphoblastic leukemia: Need for sensitive, fast, and standardized technologies. Blood **125**(26), 3996–4009 (Jun. 2015)

M.N. Dworzak et al., Standardization of flow cytometric minimal residual disease evaluation in acute lymphoblastic leukemia: Multicentric assessment is feasible. Cytometry B Clin. Cytom. **74**(6), 331–340 (2008)

G. Gaipa, G. Basso, A. Biondi, D. Campana, Detection of minimal residual disease in pediatric acute lymphoblastic leukemia. Cytom. Part B - Clin. Cytom. **84**(6), 359–369 (2013)

M. Hauwel and T. Matthes, "Minimal residual disease monitoring: The new standard for treatment evaluation of haematological malignancies?," *Swiss Medical Weekly*, vol. 144. 2014

I. Hernández-Neuta *et al.*, "Smartphone-based clinical diagnostics: towards democratization of evidence-based health care," *Journal of Internal Medicine*. 2019

W. Huang et al., *Concurrent Detection of Cellular and Molecular Cancer Markers Using an Immunomagnetic Flow System*, vol 87 (Anal. Chem, Jul. 2015), p. 10205

K. Içöz, "Image processing and cell phone microscopy to analyze the immunomagnetic beads on micro-contact printed gratings," *Appl. Sci.*, vol. 6, no. 10, 2016

K. Icoz, C. Savran, Nanomechanical biosensing with immunomagnetic separation. *Appl. Phys. Lett* **97**(12), 123701 (2010)

K. Icoz, M.C. Soylu, Z. Canikara, E. Unal, Quartz-crystal microbalance measurements of CD19 antibody immobilization on gold surface and capturing B lymphoblast cells: Effect of surface functionalization. Electroanalysis **30**(5), 834–841 (2018)

K. İçöz, T. Gerçek, A. Murat, S. Özcan, and E. Ünal, "Capturing B type acute lymphoblastic leukemia cells using two types of antibodies," *Biotechnol. Prog.*, vol. 0, no. 0

M. Islam et al., *Microfluidic Cell Sorting by Stiffness to Examine Heterogenic Responses of Cancer Cells to Chemotherapy*, vol 9 (Cell Death Dis, 2018), p. 239

J.M. Jackson et al., *Microfluidics for the Detection of Minimal Residual Disease in Acute Myeloid Leukemia Patients Using Circulating Leukemic Cells Selected from Blood*, vol 141 (Analyst, 2016), p. 640

M. Keeney, B. D. Hedley, and I. H. Chin-Yee, "Flow cytometry—Recognizing unusual populations in leukemia and lymphoma diagnosis," *International Journal of Laboratory Hematology*. 2017

P. Lucio et al., BIOMED-1 concerted action report: Flow cytometric immunophenotyping of precursor B-ALL with standardized triple-stainings. Leukemia **15**(8), 1185–1192 (Aug. 2001)

"Miltenyi Biotec."

H. Moon, J. Huh, M.S. Cho, H. Chi, W.S. Chung, *A Case of CD45-, CD19- Precursor B Cell Acute Lymphoblastic Leukemia with an Atypical Morphology*, vol 27 (Korean J. Lab. Med, 2007), p. 253

S. Nagrath et al., Isolation of rare circulating tumour cells in cancer patients by microchip technology. Nature **450**(7173), 1235–1239 (2007)

N.F. Øbro et al., *Identification of Residual Leukemic Cells by Flow Cytometry in Childhood B-Cell Precursor Acute Lymphoblastic Leukemia: Verification of Leukemic State by Flow-Sorting and Molecular/Cytogenetic Methods* (Haematologica, 2012)

A. Ozcelikkale, H.R. Moon, M. Linnes, B. Han, *In Vitro Microfluidic Models of Tumor Microenvironment to Screen Transport of Drugs and Nanoparticles*, vol 9 (Wiley Interdisciplinary Reviews, Nanomedicine and Nanobiotechnology, 2017), p. e1460

J. Rosenthal *et al.*, "Semi-Quantitative Analysis of CD19 and CD22 Expression in B-Lymphoblastic Leukemia and Implications for Targerted Immunotherapy," *Blood*, vol. 130, no. Suppl 1, 2017

R. P. Shukla, R. Cazelles, D. L. Kelly, and H. Ben-Yoav, "A reduced-graphene oxide-modified microelectrode for a repeatable detection of antipsychotic clozapine using microliters-volumes of whole blood," *Talanta*, vol. 209, no. November 2019, p. 120560, 2019

D.A. Siegel, S.J. Henley, J. Li, L.A. Pollack, E.A. Van Dyne, A. White, *Rates and Trends of Pediatric Acute Lymphoblastic Leukemia — United States, 2001–2014*, vol 66 (MMWR. Morb. Mortal. Wkly. Rep, 2017), p. 950

C. Sun et al., Immunomagnetic separation of tumor initiating cells by screening two surface markers. Sci. Rep. **7**, 40632 (2017)

T. Terwilliger and M. Abdul-Hay, "Acute Lymphoblastic Leukemia: A Comprehensive Review and 2017 Update," Blood Cancer J., 2017

F. Uslu, K. Icoz, K. Tasdemir, B. Yilmaz, Automated quantification of immunomagnetic beads and leukemia cells from optical microscope images. Biomed. Signal Process. Control **49**, 473–482 (Mar. 2019)

F. Uslu, K. Icoz, K. Tasdemir, R. S. Doğan, and B. Yilmaz, "Image-Analysis Based Readout Method for Biochip: Automated Quantification of Immunomagnetic Beads, Micropads and Patient Leukemia Cell," Micron, 2020

B. L. Wood, "Flow cytometry in the diagnosis and monitoring of acute leukemia in children," *Journal of Hematopathology*. 2015

S. Zheng et al., 3D microfilter device for viable circulating tumor cell (CTC) enrichment from blood. Biomed. Microdevices **13**(1), 203–213 (2011)